

A complete nanopore-only assembly of an XDR *Mycobacterium tuberculosis* Beijing lineage strain identifies novel genetic variation in repetitive PE/PPE gene regions

Arnold Bainomugisa^{1,2}, Tania Duarte¹, Evelyn Lavu³, Sushil Pandey⁴, Chris Coulter⁴, Ben J. Marais⁵, Lachlan Coin^{1#}

5 ¹Institute for Molecular Bioscience, The University of Queensland, Brisbane, Australia; ²Faculty
6 of Medicine, The University of Queensland, Brisbane, Australia; ³Central Public Health
7 Laboratory, Port Moresby, Papua New Guinea; ⁴Queensland Mycobacteria Reference
8 Laboratory, Brisbane, Australia; ⁵Marie Bashir Institute for Infectious diseases and Biosecurity,
9 University of Sydney, Sydney, Australia.

10

11 #Corresponding Author:

12 Assoc. Professor Lachlan Coin

13 Institute for Molecular Biosciences, The University of Queensland,

14 St Lucia, Brisbane, Australia,

15 Phone: +61733462649,

16 Email: l.coin@imb.uq.edu.au

17

18 Abstract count: 200; Main text: Word count: 3143

19 **Abstract**

20 A better understanding of the genomic changes that facilitate the emergence and spread of drug
21 resistant *M. tuberculosis* strains is required. We sequenced an extensively drug resistant (XDR)
22 Beijing sub-lineage 2.2.1.1 from the Western Province of Papua New Guinea using long-read
23 sequencing (Oxford Nanopore MinION®). We assembled a 4404947bp circular genome, with
24 3670 coding sequences including highly repetitive PE/PPE genes. Comparison with Illumina
25 reads indicated a base-level accuracy of 99.52%. Mutations known to confer drug resistance to
26 first and second line drugs were identified and concurred with phenotypic resistance assays. We
27 identified mutations in efflux pump genes (*Rv0194*), transporters (*secA1*, *glnQ*, *uspA*), cell wall
28 biosynthesis genes (*pdk*, *mmpL*, *fadD*) and virulence genes (*mce*-gene family, *mycp1*) that may
29 contribute to the drug resistance phenotype and successful transmission of this strain. Using the
30 newly assembled genome as reference to map raw Illumina reads from representative *M.*
31 *tuberculosis* lineages, we detect large insertions relative to the reference genome. We provide a
32 fully annotated genome of a transmissible XDR *M. tuberculosis* strain from Papua New Guinea
33 using Oxford Nanopore MinION sequencing and provide insight into genomic mechanisms of
34 resistance and virulence.

35 **Word count: 200**

36 **Data Summary**

- 37 1. Sample Illumina and MinION sequencing reads generated and analyzed are available in
38 NCBI under accession number SRP119110
39 (<https://www.ncbi.nlm.nih.gov/sra/?term=SRP119110>)
- 40 2. The assembled complete genome and its annotations are available in NCBI under
41 BioProject PRJNA386696
42 (<https://www.ncbi.nlm.nih.gov/bioproject/?term=PRJNA386696>)

43 **Impact statement**

44 We recently characterized a Modern Beijing lineage strain responsible for the drug resistance
45 outbreaks in the Western province, Papua New Guinea. With some of the genomic markers
46 responsible for its drug resistance and transmissibility are known, there is need to elucidate
47 all molecular mechanisms that account for the resistance phenotype, virulence and
48 transmission. Whole genome sequencing using short reads has widely been utilized to study
49 MTB genome but it does not generally capture long repetitive regions as variants in these
50 regions are eliminated using analysis. Illumina instruments are known to have a GC bias so
51 that regions with high GC or AT rich are under sampled and this effect is exacerbated in
52 MTB, which has approximately 65% GC content. In this study, we utilized Oxford
53 Nanopore Technologies (ONT) MinION sequencing to assemble a high-quality complete
54 genome of an extensively drug resistant strain of a modern Beijing lineage. We were able to
55 able to assemble all PE/PPE (proline-glutamate/proline-proline-glutamate) gene families that
56 have high GC content and repetitive in nature. We show the genomic utility of ONT in
57 offering a more comprehensive understanding of genetic mechanisms that contribute to
58 resistance, virulence and transmission. This is important for settings up predictive analytics
59 platforms and services to support diagnostics and treatment.

60 **Introduction**

61 Globally, the tuberculosis (TB) incidence rate has shown a slow decline over the last two
62 decades, although absolute case numbers continue to rise due to population growth, with an
63 estimated 10.4 million new cases occurring in 2016 (1). TB control gains are threatened by the
64 growing number of drug resistant strains recorded around the world (2). An estimated 490,000
65 incident cases of multi-drug resistant (MDR) TB, which is resistance to at least isoniazid and
66 rifampicin occurred in 2016, accounting for 374,000 deaths among HIV-positive patients (1).
67 The incidence of extensively drug resistant (XDR) strains, which are MDR strains with
68 additional resistance to at least one fluoroquinolone and second line injectable, is also on the rise
69 (3). Further multiplication of drug resistance in strains that are already highly drug resistant
70 could lead to programmatically incurable TB, where construction of a curative regimen might be
71 impossible with existing treatment options (4, 5). Management of drug resistant tuberculosis
72 places a major financial burden on health systems, which may be overwhelmed in settings with
73 high disease burdens (4).

74 In the absence of lateral gene transfer (6), drug resistance in *M. tuberculosis* arises mainly
75 from chromosomal mutations that are selected by chemotherapeutic pressure, which drives drug
76 resistance multiplication and the ongoing evolution of drug resistant strains (7-9). Successful
77 transmission of drug resistant strains results in clonal expansion and potential epidemic spread
78 (10-12). The acquisition of resistance-conferring mutations has potential for epidemic spread if
79 these drug resistant strains are readily transmissible (13, 14). The mechanisms underlying the
80 development of highly transmissible XDR strains are not fully elucidated. One such mechanism
81 is the induction of efflux pumps, which may lead to high level resistance in mycobacteria (15),
82 without any metabolic compromise. While previous studies described efflux pumps genes and

83 identified mutations in some of these genes (16, 17), efflux pump a transmissible XDR strain
84 have not been described.

85 Whole genome sequencing using short-reads has elucidated a large number of mutations
86 associated with drug resistance, as well as compensatory mutations, but has limited capacity to
87 resolve large structural variations, gene duplications or variations in repetitive regions (11, 18,
88 19). Long-read sequencing could provide a more comprehensive understanding of the
89 evolutionary mechanisms underlying the emergence of highly transmissible drug resistant strains
90 (18). In principle, Oxford nanopore MinION sequencing technology offers read lengths that are
91 only limited by the length of DNA presented and produces data in real-time (20). The small size,
92 ease of use and cheap unit cost of the Oxford MinION® nanopore sequencer facilitates successful
93 deployment in resource-limited settings, as has been achieved during the Ebola outbreak in West
94 Africa (21). Although the potential of Oxford MinION® to detect drug resistance mutations in *M.*
95 *tuberculosis* has been demonstrated, (22) its application for complete *M. tuberculosis* genome
96 assembly has not been reported.

97 Papua New Guinea (PNG) has a high rate of drug resistant TB in its Western Province (3,
98 23). We recently characterized a drug resistant tuberculosis outbreak on Daru island, which is
99 driven by a modern Beijing sub-lineage 2.2.1.1 strain (24). Whilst some genetic markers within
100 the strain have been identified (24), the molecular mechanisms responsible for pathogenesis and
101 virulence are not fully elucidated. Genomic regions like proline-glutamate (PE, 99 loci) and
102 proline-proline-glutamate (PPE, 69) genes are routinely excluded in genomic analysis of *M.*
103 *tuberculosis* due to their repetitive nature and high GC content (10, 24, 25). A recent
104 multinational study utilized 518 sample to study PE/PPE family genes and was able to assemble
105 at least 120 out of the 168 genes for each sample (26).

106 With signature motifs near the N-terminus of PE/PPE amino acids, these genes are sub
107 classified according to sequence features on the C-terminus. PE genes are divided into PE_PGRS
108 (polymorphic GC-rich sequence, 65 genes) and PE (no distinctive feature, 34 genes) while PPE
109 genes is divided into PPE_MPTR (major polymorphic tandem repeats, 23 genes), PPE_SVP
110 (Gxx-SVPxxW motif, 24 genes), PPE_PPW (PxxPxxW motif, 10 genes) and PPE (no distinctive
111 feature, 12 genes) (27). The existence of these subgroups highlights the diversity in the roles
112 played by these genes (26). PE/PPE gene products are understood to be differentially expressed
113 during infection (28) and have been implicated in immune invasion and virulence (29). We
114 utilized Oxford MinION® to compose a comprehensive draft genome of an XDR strain including
115 variable and repetitive sites like PE/PPE regions. This approach provides insight into the
116 underlying mechanisms of drug resistance and identify key features associated with virulence
117 and transmissibility. The fully assembled genome will serve as an ideal reference for ongoing
118 MDR/XDR outbreak surveillance in Western province, PNG and far north Queensland.

119 **Materials and methods**

120 ***Phenotypic susceptibility testing***

121 The strain was tested for resistance to first and second line drugs including: rifampicin
122 (1·0 µg/ml), isoniazid (0·1 µg/ml; low-level and 0·4 µg/ml; high-level), streptomycin (1·0
123 µg/ml), ethambutol (5·0 µg/ml), pyrazinamide (100 µg/ml) and second-line drugs amikacin (1·0
124 µg/ml), capreomycin (2·5 µg/ml), kanamycin (2·5 µg/ml), ethionamide (5·0 µg/ml), ofloxacin
125 (2·0 µg/ml), *p*-aminosalicylic acid (4·0 µg/ml) and cycloserine (50 µg/ml). The automated
126 Bactec Mycobacterial Growth Indicator Tube (MGIT) 960 system (Becton Dickinson, New
127 Jersey, USA) was used for first line drugs and the . Minimal inhibitory concentration assay for

128 second-line drugs was performed using Sensititre® (TREK diagnostic system, Ohio, USA)
129 system for second line drugs.

130 ***DNA extraction and quantification***

131 DNA was extracted from Lowenstein-Jensen (LJ) slopes cultured for 4 weeks at 37°C.
132 DNA isolation was performed using mechanical and chemical methods. Briefly, 5 glass beads
133 (0.7mm, SIGMA) were added to 200µl of PrepMan Ultra sample preparation reagent (Thermo
134 Fisher scientific, Massachusetts, USA). Full loops of culture were added to the reagent and
135 mixed well. The solution was dry heat incubated for 10 minutes at 95°C, followed by bead
136 beating for 40s at 6.0m/s using mini-beadbeater-16 (BioSpec products, Bartlesville, USA). It was
137 then centrifuged for 10 minutes at 13,000rpm before transferring 40µl of the supernatant into
138 another vial. We added 45µl of 3M sodium acetate and 1ml of ice-cold ethanol (96%),
139 centrifuged the solution at maximum speed for 15 minutes and removed the supernatant. We
140 then added 1 ml of 70% ethanol, left it at room temperature for 1 minute, and again removed all
141 the supernatant. The remaining pellet was dried for 15 minutes and re-suspended with 40µl of
142 nuclease free water. The DNA was quantified using Nanodrop 8000 (Thermo fisher scientific,
143 Massachusetts, USA) and Qubit dsDNA HS assay kit (Thermo fisher scientific, Massachusetts,
144 USA)

145 ***MinION® library preparation and sequencing***

146 DNA was purified using 0.4X Agencourt® AMPure® XP beads (Beckman Coulter) and
147 fragment distribution size assessed using Agilent 4200TapeStation (Agilent, UK). Preparation
148 for 1D gDNA library was performed using the SQK-LSK108 manufacturers' instructions. We
149 performed dA-tailing and end-repair using NEBNext Ultra II End-repair/dA-tail module with
150 two step incubation times; 20 minutes each. Then, purification step using 0.7X Agencourt®

151 AMPure® XP beads (Beckman Coulter) was performed according to manufacturers'
152 instructions. Ligation step was performed using NEB Blunt/ligase master mix module according
153 to manufacturers' instructions and reaction incubated at room temperature for 20 minutes.
154 Adaptor-ligated DNA was purified using 0.4X Agencourt® AMPure® XP beads (Beckman
155 Coulter) following manufacturers' instructions but using Oxford Nanopore supplied buffers
156 (adaptor bead binding and elution buffers). The library was ready for MinION® sequencing.

157 With the MinION MK1B device connected to the computer via a USB3, MinKNOW
158 software (v.1.4.3) was started to perform quality control checks on pore activity and equilibrate
159 the flow cell (FLO-MIN106, version R9.4). The library was combined with reagents supplied by
160 Oxford Nanopore and loaded onto the flow cell following manufacturers' instructions, choosing
161 a 48h sequencing procedure. Illumina data for the strain was available from our previous study.

162 ***MinION® and Illumina data analysis***

163 Raw files generated by MinKNOW were base called using Albacore (v2.0) to return
164 Oxford Nanopore Technologies (ONT) fastq files. *De novo* genome assembly was performed
165 using Canu (30) and the assembly was improved using consensus with nanopolish (31) and
166 PILON (32). The assembly was circularized using Circulator v1.5.1 (33) and compared with the
167 reference genome H37Rv (NC_000962.3) using MUMMER (34). Genome annotation was
168 performed using the NCBI pipeline (35) and circular representation of the genome viewed using
169 Circos (36). Raw ONT and Illumina reads were mapped to H37Rv using BWA-MEM (37) and
170 assessed genome and base coverage, including PE/PPE families using GATK
171 (DepthOfCoverage) (38). We assessed single nucleotide polymorphisms (SNPs) within PE/PPE
172 genes from nanopore and Illumina reads. In addition, representative raw Illumina reads from four
173 *M. tuberculosis* lineages; Indo-Oceanic, East-Asian (including Beijing lineage), East-African-

174 Indian and Euro-American lineage (including H37Rv) from previous studies (25, 39-41) were
175 mapped to the draft genome and assessed for large deletions that differentiate the draft genome
176 from other lineages.

177 ***MinION variant and error analysis***

178 Using the reference genome H37Rv (NC_000962.3), single nucleotide polymorphisms
179 (SNPs) and small indels (<5bp) were called from ONT reads using nanoprocess (31) and
180 annotated using SnpEff (42). Polymorphisms in known drug resistance genes (including
181 compensatory mutations) were analyzed. MycoBrowser (43) was utilized to analyze mutations in
182 genes that are putatively involved in virulence, efflux pumps and cell transport. Illumina reads of
183 the same strain were mapped onto the reference genome and variants called using GATK (38).
184 Consensus SNPs from the two methods were assessed and ‘non-consensus SNPs’ from ONT
185 reads were considered sequencing errors provided Illumina coverage was greater than 30X. This
186 analysis excluded SNPs in variable regions like PE/PPE genes. Different software to generate
187 variants from ONT and Illumina raw files was combined into an analysis pipeline (Fig. S1).

188 **Results**

189 In total, 373952 ONT reads passed base calling with N50 read length of 5073bp. The
190 longest read was 33509bp. Genome assembly resulted in one contig of 4404947bp (G+C content
191 65.5%), with base consistency similar to H37Rv (NC_000962.3) (Fig. S2). NCBI annotation of
192 the genome yielded a total of 3,670 coding DNA sequences (CDS), 45 tRNAs, 3 rRNAs (5S,
193 16S, 23S) and 3 non-coding RNA (Fig. 1). Mapping of the ONT reads to H37Rv resulted in a
194 coverage of 98.4% at average read depth of 273x (Table S1). Nearly all PE/PPE genes (167/168)
195 were completely assembled with 100% coverage; only one (*wag22*; RV1759c) had incomplete
196 (88%) coverage in our assembly relative to H37Rv. The average ONT read depth of PE/PPE

197 genes was 299.87 (IQR 285.91-311.36) (Fig. S3). Only 54.3% (92/168) of the PE/PPE genes
198 were completely assembled from Illumina contigs at average sequence depth of x46.3 (Fig. S4).
199 No Illumina reads covered the PE_PGRS sub-family genes *wag22* and PE_PGRS57.

200 We first evaluated SNP calling in the non-repetitive part of the reference genome by
201 excluding variable (PE/PPE) regions. A total of 1254 SNPs and 122 small indels were called
202 from ONT reads while 1098 SNPs and 105 small indels were called from Illumina reads when
203 mapped to H37Rv. Of these, 1095 SNPs (574 non-synonymous and 402 synonymous) and 87
204 small indels were identified by both approaches. 118 of 159 SNPs and 23 of 35 indels identified
205 from MinION® but not Illumina were in regions of low Illumina coverage (<30x coverage). The
206 remaining 41 and 12 SNPs and Indels respectively are potentially due to systematic base-calling
207 errors (3.2% and 9.8 %). Three (0.2%) SNPs and 18 (14.7%) indels were identified by Illumina,
208 but not by MinION® sequencing. As a conservative estimate considering all 194 ONT only calls
209 (159 SNPs and 35 indels) as false positives and 21 Illumina only calls (3 SNPs and 18 Indels) as
210 false negative, the error rate after consensus calling from ONT was 0.0048. If we ignore
211 inconsistent calls where Illumina coverage was low then the estimated error rate for base calling
212 from ONT was reduced to 0.0036

213 Given the likely importance of the variable PE/PPE genes in strain evolution we assessed
214 the ability of MinION® and Illumina to call SNPs in this class of genes separately. From
215 nanopore assembly, 158 SNPs were identified from 70 PE/PPE genes (42 PE and 28 PPE) with
216 88 SNPs (55.6%) identified from the PE_PGRS sub-family (Table S2). From the Illumina
217 assembly, 124 SNPs from 45 PE/PPE genes (25 PE and 20 PPE) were identified of which 31
218 SNPs (25%) were from PE_PGRS sub-family. There were 81 SNPs (from 42 PE/PPE genes)

219 overlapping between ONT and Illumina with PPE54 having the highest number of overlapped
220 SNPs (9) identified within one gene.

221 Phenotypic drug susceptibility results revealed the isolate to be extensively drug resistant
222 with susceptibility to only amikacin, kanamycin, para-aminosalicylic acid (PAS) and
223 cycloserine. Table 1 reflects phenotypic resistance, as well as mutations in genes known to
224 confer drug resistance to first and second line drugs and recognized compensatory mutations.
225 Genotypic drug resistance profiles concurred with phenotypic results. While 10 mutations were
226 identified in seven genes that encode trans-membrane efflux pumps and transporter proteins
227 (Table 2). Table 3 shows 16 SNPs identified in genes that encode virulence proteins; 8 (50%)
228 were from the *mce*-gene family and a mutation within *mycP1* (p.Thr238Ala) was also noted. In
229 addition, 27 SNPs were identified in three genes families involved in cell wall synthesis, with 17
230 in *fadD*, 4 in *pks* and 3 in *mmp* gene families (Table S3).

231 Mapping of raw sequence reads from representative lineage 1 (Indo-Oceanic), 2 (East
232 Asian, including ancient and modern Beijing), 3 (East-African-Indian) and 4 (Euro-American,
233 including H37Rv) strains identified a 4490bp (2207042-2211532) region absent in Euro-
234 American lineage strains (Fig. 2). Three previously assembled Beijing genomes from PacBio
235 long reads identified the same region (41) (Fig. S5). Like in previous studies (44-46), annotation
236 of this region was revealed to span 7 complete genes that encode proteins that include a
237 nicotinamide adenine dinucleotide phosphate (NADP)-dependent oxidoreductase, an iron-
238 regulated elongation factor (Tu), a PE-family protein while four genes encode uncharacterized
239 proteins (Fig. 2).

240 A second smaller insertion (390bp, 3488211-3488601) was identified among Beijing
241 lineage genomes relative to H37Rv and Euro-American lineages but varied in size as it was

242 835bp with respect to Indo-oceanic and East-African-Indian lineages (Fig. 2). Annotation
243 showed a 654bp gene (3487881-3488534) in this region had part of the insertion sequence,
244 323bp (3488211-3488534) towards the end. Phyre2 protein modelling (47) of the gene sequence
245 with the insertion revealed PE8-PPE15 as template to construct to predict the protein structure as
246 a PPE family protein (79% sequence modelled, 100% confidence) consisting of 73% alpha
247 helices (Fig. S6). A blast search of this gene sequence revealed a 50% query coverage to four
248 *Mycobacterium tuberculosis* H37Rv genomes (100% identification) and 100% query coverage to
249 55 *Mycobacterium tuberculosis*, Lineage 2 genomes (Table S4).

250 **Discussion**

251 In this study, we utilized Oxford Nanopore MinION sequencing to assemble a
252 comprehensive genome of a strain that is responsible for a drug resistant outbreaks in the
253 Western Province of Papua New Guinea (24). The complete circular genome of this modern
254 Beijing sub-lineage 2.2.1.1 strain revealed genetic determinants of drug resistance against first
255 and second line TB drugs. Nanopore sequencing allowed us to assemble highly variable PE/PPE
256 gene families with great fidelity. PE/PPE genes are thought to encode surface-associated cell
257 wall proteins that may provide antigenic diversity and affect host immunity (28). Nanopore
258 technology has been previously used to improve genome assemblies and resolution of repeat-rich
259 regions in *Salmonella typhi* and *Escherichia coli* (19, 31) but not yet with *Mycobacterium*
260 *tuberculosis*.

261 Twice as many SNPs in PE_PGRS genes were identified as by ONT Minion versus
262 Illumina sequencing (88 vs 31). PE_PGRS gene mutations were under-represented in short-read
263 sequencing, possibly due to their extra GC containing motifs that impact on the sequencing.
264 Previous studies have identified a higher number of mutations within the PE_PGRS sub-family

265 compared to other PE subfamilies, and attribute it to their involvement in antigenic variation and
266 immune evasion from exposure to host immune system (26, 48). The *wag22* gene was also
267 better represented by nanopore sequencing, with 88% coverage compared to no coverage from
268 Illumina reads. Besides the high GC content, the difficulty of sequencing *wag22* has been further
269 attributed to deletions at the beginning of the open reading frame (48). Unsurprisingly, PPE54
270 which is a member of PPE_MPTR (major polymorphic tandem repeat) sub-family had the
271 highest number of mutations from ONT sequence. Previous studies have shown it to be involved
272 in the ‘arrest’ of phagosome maturation to allow survival of the bacteria in the macrophages due
273 to its long amino acid length at the C-terminal (49, 50). It has been postulated that PPE54 gene
274 mutations may also play a role in development of isoniazid, rifampicin and ethambutol resistance
275 (51), but we were unable to verify this given the presence of well-characterized drug resistance
276 mutations.

277 There is growing interest in using Oxford Nanopore Technologies devices for real-time
278 clinical utility as a cheap point-of-care TB diagnostic, with accurate identification of
279 antimicrobial resistance profiles. Sequencing for drug resistance mutations directly from clinical
280 samples has been completed within a 24 hours in patients with sputum smear-positive
281 tuberculosis(22). In our study, nanopore sequencing of an XDR strain fully identified its drug
282 resistance profile with complete phenotypic concordance. We were able to identify all relevant
283 first line and second line drug resistance conferring SNPs using Oxford nanopore MinION
284 sequencing. Compensatory mutations also detected in genes like *rpoC* (p.Val483Gly) and *ndh*
285 (c.304delG) are thought to ameliorate the fitness cost associated with the XDR phenotype (39,
286 52).

287 We also identified mutations in efflux pumps and transporter proteins, which might
288 contribute to resistance phenotypes (53). Mutations in transporter proteins like ABC (ATP
289 binding cassette) and MFS (Major Facilitator Super family) have been associated with drug
290 resistance (54, 55). For example, mutations leading to overexpression of the ABC transporter
291 Rv0194 leads to increased export of multiple drugs like streptomycin, vancomycin, and
292 tetracycline (56). We identified two mutations in *uspA*, which is part of the three gene operon
293 *uspABC* that encodes membrane-spanning subunits transporting amino-sugar substrates across
294 the cell wall (57). Mutations found in Rv0194 have been associated with resistance to beta
295 lactams antibiotics (56) and its over expression with an XDR phenotype (58). Further research
296 needs to be done to explore the association between efflux pump mutations, pump activity and
297 drug resistance.

298 Mutations in co-localized genes like; *mmpL*, *pks* and *fadd* have been considered to play
299 a compensatory role to restore the fitness of drug resistant strains (59, 60) especially for drugs
300 that target biosynthesis pathways of the mycobacterial cell wall like isoniazid, ethionamide (6)
301 and ethambutol (61). *M. tuberculosis* contains 13 genes that encode *mmpL* proteins and 16 genes
302 that encode polyketide synthases (*pks*) proteins that are involved in lipopolysaccharide and
303 complex lipid biosynthesis. The functional cross talk between *pks* and *fadd* genes has been
304 demonstrated in studies that showed how *pks13* and *fad32* form specific substrates that are
305 precursors of mycolic acid biosynthesis (62). We identified mutations in all three genes although
306 there was greater mutation variability within *fadd* genes. It remains to be determined how
307 mutations in these co-localized genes influence cell wall lipid biosynthesis.

308 Insight into the factors that influence mycobacterial virulence is important for better
309 appreciation of microbial pathogenesis and the identification of new treatment options. SNPs in

310 mammalian cell entry (*mce*) genes were prominent. *Mce*-family proteins are proposed to be
311 involved in invasion and persistence of *M. tuberculosis* in host macrophages (63). This is related
312 to the ability of these cell surface proteins to mediate bacterial uptake by mammalian cells,
313 similar to those stimulated by invasive enteric bacteria (64). It has been demonstrated that a
314 mutant *mce1A* *M. tuberculosis* strain is “hyper virulent” in mice (65). Comparative analysis
315 among different *M. tuberculosis* strains could unveil characteristics related to host adaption (66).

316 Although *M. tuberculosis* has relatively limited genetic variation compared to other
317 pathogenic bacteria, there is strain-related phenotypic variation in the protection provided by
318 Bacille Calmette-Guerin (BCG) vaccination and clinical outcome (67). We didn’t find any large
319 indel (>1kb) unique to the study strain but identified a large region (4490bp) with 7 coding
320 sequences present in the draft genome and other reference genomes (lineage 1, 2 and 3) but
321 absent in lineage 4 genomes including H37Rv. These have been previously described (44-46)
322 and this further demonstrates the limitations of using H37Rv as the universal reference strain.
323 The second smaller region within the draft genome but with variable sizes among the reference
324 genomes highlights evidence of independent structural rearrangement among the different
325 lineages. The identified PPE family protein unique to Beijing lineage 2 could contribute to
326 phenotypic characteristics of this lineage. Such a comparative approach provides an opportunity
327 to study lineage and strain specific differences, especially in the advent of long read sequencing
328 with enhanced resolution of variable parts of the genome.

329 In conclusion, the assembly of a complete genome of a XDR “epidemic strain” using
330 nanopore technology did not only provide proof of principle for future deployment of this
331 technology in settings endemic for drug resistant tuberculosis but it also demonstrated the use of
332 this technology in further understanding of *M. tuberculosis* genetics. It characterized the drug

333 resistance profile and potential virulence factors found in this strain, and provided a reference
334 strain for future genome assembly and mapping.

335 **Data bibliography**

336 1. NCBI accession number SRP119110, CP022704 (2018)
337 2. GenBank accession numbers AP018034 (HN-205), AP018035 (HN-321), and
338 AP018036(HN-506)-2017

339 **Funding**

340 This study was supported by funding from the Centre for Superbugs Solutions (610246),
341 Institute for Molecular Bioscience.

342 **Ethic statement**

343 The isolate was selected from a previous study (24) with ethics clearance from the
344 University of Queensland and the Papua New Guinea Medical Research Advisory Committee to
345 perform detailed whole genome sequencing.

346 **Acknowledgements**

347 We thank the Papua New Guinea National Tuberculosis Program, Provincial Health Staff
348 (Western Province) and staff of Queensland Mycobacterium Reference Laboratory for their
349 assistance. This research was supported by the use of the NeCTAR Research Cloud, by QCIF
350 and by the University of Queensland's Research Computing Centre (RCC). The NeCTAR
351 Research Cloud is a collaborative Australian research platform supported by the National
352 Collaborative Research Infrastructure Strategy.

353 **References**

- 354 1. WHO. GLOBAL TUBERCULOSIS REPORT 2016. Switzerland: World Health
355 Organization, Geneva, 2017.
- 356 2. Abubakar I, Zignol M, Falzon D, Raviglione M, Ditiu L, Masham S, et al. Drug-resistant
357 tuberculosis: time for visionary political leadership. *The Lancet Infectious diseases*.
358 2013;13(6):529-39.
- 359 3. World Health Organization., Global Tuberculosis Programme. Global tuberculosis
360 control : WHO report. Geneva: Global Tuberculosis Programme. p. 15 volumes.
- 361 4. Dheda K, Gumbo T, Maartens G, Dooley KE, McNerney R, Murray M, et al. The
362 epidemiology, pathogenesis, transmission, diagnosis, and management of multidrug-resistant,
363 extensively drug-resistant, and incurable tuberculosis. *The Lancet Respiratory medicine*. 2017.
- 364 5. Udwadia ZF. MDR, XDR, TDR tuberculosis: ominous progression. *Thorax*.
365 2012;67(4):286-8.
- 366 6. Zhang Y, Yew WW. Mechanisms of drug resistance in *Mycobacterium tuberculosis*:
367 update 2015. *The international journal of tuberculosis and lung disease : the official journal of*
368 *the International Union against Tuberculosis and Lung Disease*. 2015;19(11):1276-89.
- 369 7. Eldholm V, Monteserin J, Rieux A, Lopez B, Sobkowiak B, Ritacco V, et al. Four
370 decades of transmission of a multidrug-resistant *Mycobacterium tuberculosis* outbreak strain.
371 *Nature communications*. 2015;6:7119.
- 372 8. Ioerger TR, Feng Y, Chen X, Dobos KM, Victor TC, Streicher EM, et al. The non-
373 clonality of drug resistance in Beijing-genotype isolates of *Mycobacterium tuberculosis* from the
374 Western Cape of South Africa. *BMC genomics*. 2010;11:670.

- 375 9. Didelot X, Walker AS, Peto TE, Crook DW, Wilson DJ. Within-host evolution of
376 bacterial pathogens. *Nature reviews Microbiology*. 2016;14(3):150-62.
- 377 10. Cohen KA, Abeel T, Manson McGuire A, Desjardins CA, Munsamy V, Shea TP, et al.
378 Evolution of Extensively Drug-Resistant Tuberculosis over Four Decades: Whole Genome
379 Sequencing and Dating Analysis of *Mycobacterium tuberculosis* Isolates from KwaZulu-Natal.
380 *PLoS medicine*. 2015;12(9):e1001880.
- 381 11. Casali N, Nikolayevskyy V, Balabanova Y, Harris SR, Ignatyeva O, Kontsevaya I, et al.
382 Evolution and transmission of drug-resistant tuberculosis in a Russian population. *Nature*
383 *genetics*. 2014;46(3):279-86.
- 384 12. Casali N, Nikolayevskyy V, Balabanova Y, Ignatyeva O, Kontsevaya I, Harris SR, et al.
385 Microevolution of extensively drug-resistant tuberculosis in Russia. *Genome research*.
386 2012;22(4):735-45.
- 387 13. McBryde ES, Meehan MT, Doan TN, Ragonnet R, Marais BJ, Guernier V, et al. The risk
388 of global epidemic replacement with drug-resistant *Mycobacterium tuberculosis* strains.
389 *International journal of infectious diseases : IJID : official publication of the International*
390 *Society for Infectious Diseases*. 2017;56:14-20.
- 391 14. Marais BJ, Mlambo CK, Rastogi N, Zozio T, Duse AG, Victor TC, et al. Epidemic
392 spread of multidrug-resistant tuberculosis in Johannesburg, South Africa. *Journal of clinical*
393 *microbiology*. 2013;51(6):1818-25.
- 394 15. Schmalstieg AM, Srivastava S, Belkaya S, Deshpande D, Meek C, Leff R, et al. The
395 antibiotic resistance arrow of time: efflux pump induction is a general first step in the evolution
396 of mycobacterial drug resistance. *Antimicrobial agents and chemotherapy*. 2012;56(9):4806-15.

- 397 16. Garima K, Pathak R, Tandon R, Rathor N, Sinha R, Bose M, et al. Differential expression
398 of efflux pump genes of *Mycobacterium tuberculosis* in response to varied subinhibitory
399 concentrations of antituberculosis agents. *Tuberculosis*. 2015;95(2):155-61.
- 400 17. Ali A, Hasan Z, McNerney R, Mallard K, Hill-Cawthorne G, Coll F, et al. Whole genome
401 sequencing based characterization of extensively drug-resistant *Mycobacterium tuberculosis*
402 isolates from Pakistan. *PLoS one*. 2015;10(2):e0117771.
- 403 18. Didelot X, Bowden R, Wilson DJ, Peto TEA, Crook DW. Transforming clinical
404 microbiology with bacterial genome sequencing. *Nature reviews Genetics*. 2012;13(9):601-12.
- 405 19. Ashton PM, Nair S, Dallman T, Rubino S, Rabsch W, Mwaigwisya S, et al. MinION
406 nanopore sequencing identifies the position and structure of a bacterial antibiotic resistance
407 island. *Nature biotechnology*. 2015;33(3):296-300.
- 408 20. Laver T, Harrison J, O'Neill PA, Moore K, Farbos A, Paszkiewicz K, et al. Assessing the
409 performance of the Oxford Nanopore Technologies MinION. *Biomolecular detection and*
410 *quantification*. 2015;3:1-8.
- 411 21. Quick J, Loman NJ, Duraffour S, Simpson JT, Severi E, Cowley L, et al. Real-time,
412 portable genome sequencing for Ebola surveillance. *Nature*. 2016;530(7589):228-32.
- 413 22. Votintseva AA, Bradley P, Pankhurst L, Del Ojo Elias C, Loose M, Nilgiriwala K, et al.
414 Same-Day Diagnostic and Surveillance Data for Tuberculosis via Whole-Genome Sequencing of
415 Direct Respiratory Samples. *Journal of clinical microbiology*. 2017;55(5):1285-98.
- 416 23. Aia P, Kal M, Lavu E, John LN, Johnson K, Coulter C, et al. The Burden of Drug-
417 Resistant Tuberculosis in Papua New Guinea: Results of a Large Population-Based Survey. *PLoS*
418 *one*. 2016;11(3):e0149806.

- 419 24. Bainomugisa A, Lavu E, Hiashiri S, Majumdar S, Honjepari A, Moke R, et al. Multi-
420 clonal evolution of multi-drug-resistant/extensively drug-resistant *Mycobacterium tuberculosis*
421 in a high-prevalence setting of Papua New Guinea for over three decades. *Microbial genomics*.
422 2018.
- 423 25. Merker M, Blin C, Mona S, Duforet-Frebourg N, Lecher S, Willery E, et al. Evolutionary
424 history and global spread of the *Mycobacterium tuberculosis* Beijing lineage. *Nature genetics*.
425 2015;47(3):242-9.
- 426 26. Phelan JE, Coll F, Bergval I, Anthony RM, Warren R, Sampson SL, et al. Recombination
427 in pe/ppe genes contributes to genetic variation in *Mycobacterium tuberculosis* lineages. *BMC*
428 *genomics*. 2016;17:151.
- 429 27. Fishbein S, van Wyk N, Warren RM, Sampson SL. Phylogeny to function: PE/PPE
430 protein evolution and impact on *Mycobacterium tuberculosis* pathogenicity. *Molecular*
431 *microbiology*. 2015;96(5):901-16.
- 432 28. Mohareer K, Tundup S, Hasnain SE. Transcriptional regulation of *Mycobacterium*
433 tuberculosis PE/PPE genes: a molecular switch to virulence? *Journal of molecular microbiology*
434 and biotechnology. 2011;21(3-4):97-109.
- 435 29. Singh KK, Zhang X, Patibandla AS, Chien P, Jr., Laal S. Antigens of *Mycobacterium*
436 tuberculosis expressed during preclinical tuberculosis: serological immunodominance of proteins
437 with repetitive amino acid sequences. *Infection and immunity*. 2001;69(6):4185-91.
- 438 30. Koren S, Walenz BP, Berlin K, Miller JR, Bergman NH, Phillippy AM. Canu: scalable
439 and accurate long-read assembly via adaptive k-mer weighting and repeat separation. *Genome*
440 *research*. 2017;27(5):722-36.

- 441 31. Loman NJ, Quick J, Simpson JT. A complete bacterial genome assembled de novo using
442 only nanopore sequencing data. *Nature methods*. 2015;12(8):733-5.
- 443 32. Walker BJ, Abeel T, Shea T, Priest M, Abouelliel A, Sakthikumar S, et al. Pilon: an
444 integrated tool for comprehensive microbial variant detection and genome assembly
445 improvement. *PLoS one*. 2014;9(11):e112963.
- 446 33. Hunt M, Silva ND, Otto TD, Parkhill J, Keane JA, Harris SR. Circlator: automated
447 circularization of genome assemblies using long sequencing reads. *Genome biology*.
448 2015;16:294.
- 449 34. Kurtz S, Phillippy A, Delcher AL, Smoot M, Shumway M, Antonescu C, et al. Versatile
450 and open software for comparing large genomes. *Genome biology*. 2004;5(2):R12.
- 451 35. Angiuoli SV, Gussman A, Klimke W, Cochrane G, Field D, Garrity G, et al. Toward an
452 online repository of Standard Operating Procedures (SOPs) for (meta)genomic annotation.
453 *Omics : a journal of integrative biology*. 2008;12(2):137-41.
- 454 36. Krzywinski M, Schein J, Birol I, Connors J, Gascoyne R, Horsman D, et al. Circos: an
455 information aesthetic for comparative genomics. *Genome research*. 2009;19(9):1639-45.
- 456 37. Li H. Aligning sequence reads, clone sequences and assembly contigs with BWA-MEM.
457 *arXiv*. 2013;:1303.3997v1 [q-bio.GN].
- 458 38. McKenna N, Hanna M, Banks E, Sivachenko A, Cibulskis K, Kernytsky A, et al. The
459 Genome Analysis Toolkit: a MapReduce framework for analyzing next-generation DNA
460 sequencing data. *Genome research*. 2010;20(9):1297-303.
- 461 39. Bainomugisa A, Lavu E, Hiashiri S, Majumdar S, Honjepari A, Moke R, et al. Multi-
462 clonal evolution of MDR/XDR *M. tuberculosis* in a high prevalence setting in Papua New
463 Guinea over three decades. *bioRxiv*. 2017.

- 464 40. Guerra-Assuncao JA, Crampin AC, Houben RM, Mzembe T, Mallard K, Coll F, et al.
- 465 Large-scale whole genome sequencing of *M. tuberculosis* provides insights into transmission in a
- 466 high prevalence area. *eLife*. 2015;4.
- 467 41. Wada T, Hijikata M, Maeda S, Hang NTL, Thuong PH, Hoang NP, et al. Complete
- 468 Genome Sequences of Three Representative *Mycobacterium tuberculosis* Beijing Family Strains
- 469 Belonging to Distinct Genotype Clusters in Hanoi, Vietnam, during 2007 to 2009. *Genome*
- 470 announcements. 2017;5(27).
- 471 42. Cingolani P, Platts A, Wang le L, Coon M, Nguyen T, Wang L, et al. A program for
- 472 annotating and predicting the effects of single nucleotide polymorphisms, SnpEff: SNPs in the
- 473 genome of *Drosophila melanogaster* strain w1118; iso-2; iso-3. *Fly*. 2012;6(2):80-92.
- 474 43. Kapopoulou A, Lew JM, Cole ST. The MycoBrowser portal: a comprehensive and
- 475 manually annotated resource for mycobacterial genomes. *Tuberculosis*. 2011;91(1):8-13.
- 476 44. Periwal V, Patowary A, Vellarikkal SK, Gupta A, Singh M, Mittal A, et al. Comparative
- 477 whole-genome analysis of clinical isolates reveals characteristic architecture of *Mycobacterium*
- 478 tuberculosis pangenome. *PloS one*. 2015;10(4):e0122979.
- 479 45. O'Toole RF, Gautam SS. Limitations of the *Mycobacterium tuberculosis* reference
- 480 genome H37Rv in the detection of virulence-related loci. *Genomics*. 2017.
- 481 46. Gautam SS, Mac Aogain M, Bower JE, Basu I, O'Toole RF. Differential carriage of
- 482 virulence-associated loci in the New Zealand Rangipo outbreak strain of *Mycobacterium*
- 483 tuberculosis. *Infectious diseases*. 2017;49(9):680-8.
- 484 47. Kelley LA, Mezulis S, Yates CM, Wass MN, Sternberg MJ. The Phyre2 web portal for
- 485 protein modeling, prediction and analysis. *Nature protocols*. 2015;10(6):845-58.

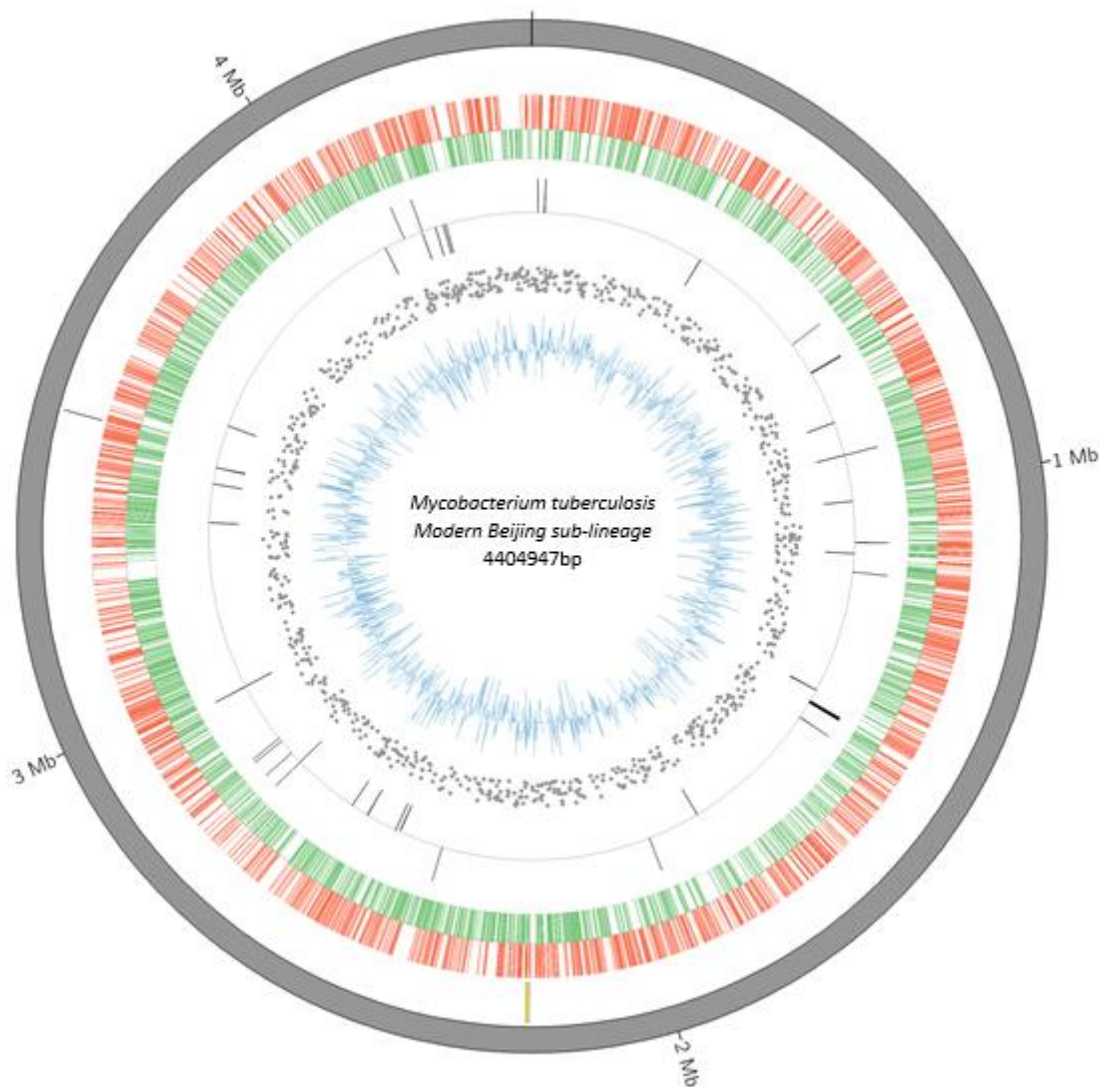
- 486 48. Copin R, Coscolla M, Seiffert SN, Bothamley G, Sutherland J, Mbayo G, et al. Sequence
487 diversity in the pe_pgrs genes of *Mycobacterium tuberculosis* is independent of human T cell
488 recognition. *mBio*. 2014;5(1):e00960-13.
- 489 49. Sampson SL. Mycobacterial PE/PPE proteins at the host-pathogen interface. *Clinical &*
490 *developmental immunology*. 2011;2011:497203.
- 491 50. Brodin P, Poquet Y, Levillain F, Peguillet I, Larrouy-Maumus G, Gilleron M, et al. High
492 content phenotypic cell-based visual screen identifies *Mycobacterium tuberculosis* acyltrehalose-
493 containing glycolipids involved in phagosome remodeling. *PLoS pathogens*.
494 2010;6(9):e1001100.
- 495 51. Cui ZJ, Yang QY, Zhang HY, Zhu Q, Zhang QY. Bioinformatics Identification of Drug
496 Resistance-Associated Gene Pairs in *Mycobacterium tuberculosis*. *International journal of*
497 *molecular sciences*. 2016;17(9).
- 498 52. Comas I, Borrell S, Roetzer A, Rose G, Malla B, Kato-Maeda M, et al. Whole-genome
499 sequencing of rifampicin-resistant *Mycobacterium tuberculosis* strains identifies compensatory
500 mutations in RNA polymerase genes. *Nature genetics*. 2012;44(1):106-10.
- 501 53. Kanji A, Hasan R, Zhang Y, Shi W, Imtiaz K, Iqbal K, et al. Increased expression of
502 efflux pump genes in extensively drug-resistant isolates of *Mycobacterium tuberculosis*.
503 *International journal of mycobacteriology*. 2016;5 Suppl 1:S150.
- 504 54. Liu J, Takiff HE, Nikaido H. Active efflux of fluoroquinolones in *Mycobacterium*
505 *smegmatis* mediated by LfrA, a multidrug efflux pump. *Journal of bacteriology*.
506 1996;178(13):3791-5.

- 507 55. De Rossi E, Arrigo P, Bellinzoni M, Silva PA, Martin C, Ainsa JA, et al. The multidrug
508 transporters belonging to major facilitator superfamily in *Mycobacterium tuberculosis*.
509 *Molecular medicine*. 2002;8(11):714-24.
- 510 56. Danilchanka O, Mailaender C, Niederweis M. Identification of a novel multidrug efflux
511 pump of *Mycobacterium tuberculosis*. *Antimicrobial agents and chemotherapy*.
512 2008;52(7):2503-11.
- 513 57. Fullam E, Prokes I, Futterer K, Besra GS. Structural and functional analysis of the solute-
514 binding protein UspC from *Mycobacterium tuberculosis* that is specific for amino sugars. *Open*
515 *biology*. 2016;6(6).
- 516 58. Kanji A, Hasan R, Ali A, Zaver A, Zhang Y, Imtiaz K, et al. Single nucleotide
517 polymorphisms in efflux pumps genes in extensively drug resistant *Mycobacterium tuberculosis*
518 isolates from Pakistan. *Tuberculosis*. 2017;107(Supplement C):20-30.
- 519 59. Zhang H, Li D, Zhao L, Fleming J, Lin N, Wang T, et al. Genome sequencing of 161
520 *Mycobacterium tuberculosis* isolates from China identifies genes and intergenic regions
521 associated with drug resistance. *Nature genetics*. 2013;45(10):1255-60.
- 522 60. Kuan CS, Chan CL, Yew SM, Toh YF, Khoo JS, Chong J, et al. Genome Analysis of the
523 First Extensively Drug-Resistant (XDR) *Mycobacterium tuberculosis* in Malaysia Provides
524 Insights into the Genetic Basis of Its Biology and Drug Resistance. *PloS one*.
525 2015;10(6):e0131694.
- 526 61. Birch HL, Alderwick LJ, Bhatt A, Rittmann D, Krumbach K, Singh A, et al. Biosynthesis
527 of mycobacterial arabinogalactan: identification of a novel alpha(1-->3)
528 arabinofuranosyltransferase. *Molecular microbiology*. 2008;69(5):1191-206.

- 529 62. Gavalda S, Leger M, van der Rest B, Stella A, Bardou F, Montrozier H, et al. The
530 Pks13/FadD32 crosstalk for the biosynthesis of mycolic acids in *Mycobacterium tuberculosis*.
531 *The Journal of biological chemistry*. 2009;284(29):19255-64.
- 532 63. Casali N, Riley LW. A phylogenomic analysis of the Actinomycetales mce operons.
533 *BMC genomics*. 2007;8:60.
- 534 64. Bliska JB, Galan JE, Falkow S. Signal transduction in the mammalian cell during
535 bacterial attachment and entry. *Cell*. 1993;73(5):903-20.
- 536 65. Shimono N, Morici L, Casali N, Cantrell S, Sidders B, Ehrt S, et al. Hypervirulent mutant
537 of *Mycobacterium tuberculosis* resulting from disruption of the mce1 operon. *Proceedings of the*
538 *National Academy of Sciences of the United States of America*. 2003;100(26):15918-23.
- 539 66. Cubillos-Ruiz A, Morales J, Zambrano MM. Analysis of the genetic variation in
540 *Mycobacterium tuberculosis* strains by multiple genome alignments. *BMC research notes*.
541 2008;1:110.
- 542 67. Gagneux S, Small PM. Global phylogeography of *Mycobacterium tuberculosis* and
543 implications for tuberculosis product development. *The Lancet Infectious diseases*.
544 2007;7(5):328-37.
- 545

546 **Figures and tables**

547 **Main text**



548

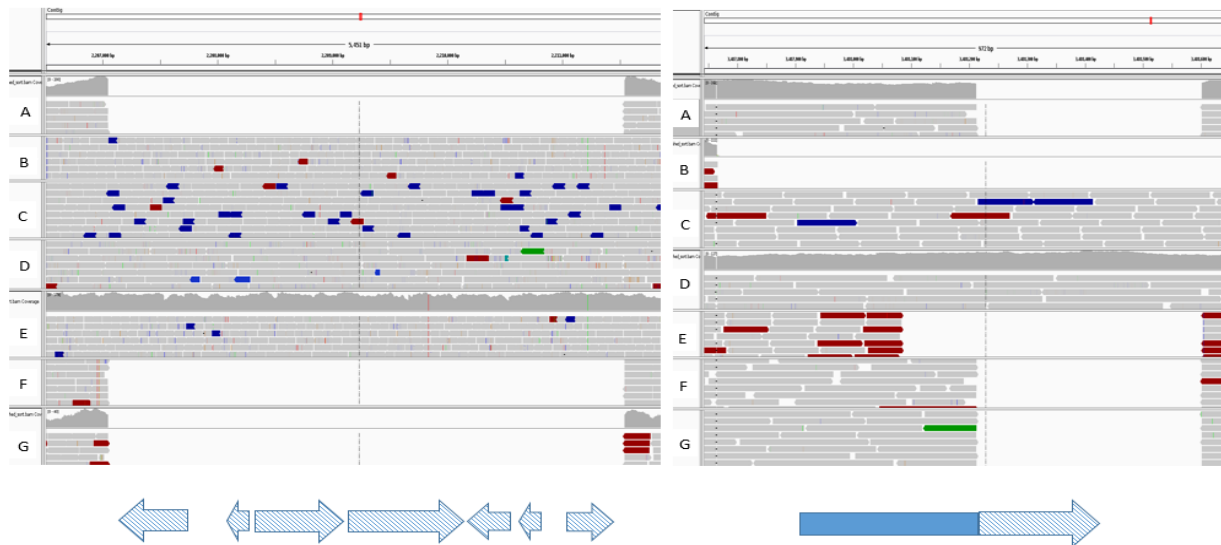
549 **Fig. 1:** Circular representation of the drafted XDR genome from Western Province, Papua New
550 Guinea (modern Beijing sub-lineage 2.2.1.1 strain) with gene annotations. From the inner to
551 outer ring: Blue - GC content of coding sequence; Scattered grey - SNPs relative to H37Rv; Grey
552 bars - reverse and forward *rRNA*; Green - reverse coding sequences; Red - forward coding

553 sequences; Yellow bars - unique regions compared to H37Rv; Grey outside ring - assembled

554 contig (grey). Mb-million base pairs; XDR – extensively drug resistant

555

556



557

558 **Fig. 2:** Integrative Genomic Viewer (IGV) of Illumina reads from different *M. tuberculosis*
559 lineages (A- *M. tuberculosis* H37Rv, B-Indo-oceanic, C-Ancient Beijing, D-Modern Beijing, E-
560 East African Indian, F&G-Euro American) mapped on the ONT draft genome highlighting the
561 large insertions within the draft genome. On the left-4490bp insertion (2207042-2211532)
562 spanning 7 annotated genes (blue checked arrows-NADH-dependent oxidoreducatse, Iron-
563 regulated elongation factor-tu, PE family protein and hypothetical/uncharacterized proteins). On
564 the right-390bp insertion relative to H37Rv (3488211-3488601) spanning 323bp (checked) at the
565 end of a 654bp coding sequence. ONT – Oxford Nanopore Technologies

566 **Table 1:** Mutations in candidate drug resistance genes identified from ONT assembly of XDR
567 Beijing sub-lineage 2.2.1.1 strain

Drug	Invitro phenotype	Investigated genes	Genes (mutation)
Isoniazid	Resistant	<i>fabG1-inhA, inhA, katG, ndh, furA, oxyR, aphC, fadE24, srmR, kasA, mshA</i>	<i>fabG1-inhA (C-15T)</i>
		<i>inhA (p.Ile21Val)</i>	
		<i>ndh (delG304)</i>	
Rifampicin	Resistant	<i>rpoB, rpoC, rpoA, rpoD</i>	<i>rpoB (p.Ser450Leu)</i>
		<i>rpoC (p.Val483Gly)</i>	
Ethambutol	Resistant	<i>embB, embC, embA, ubiA, embR, iniA, iniC, manB</i>	<i>embB (p.Met306Val)</i>
Pyrazinamide	Resistant	<i>pncA, rpsA, panD</i>	<i>pncA(p.Tyr103Asp)</i>
Streptomycin	Resistant	<i>rpsL, gidB, rrs</i>	<i>rpsL (p.Lys43Arg)</i>
		<i>gidB (p.Leu91Pro)</i>	
Ethionamide	Resistant	<i>fabG1-inhA, ethA, ethR</i>	<i>fabG1-inhA(C-15T)</i>
Fluoroquinolone	Resistant	<i>gyrA, gyrB</i>	<i>gyrA (p.Asp94Gly)</i>
Amikacin	Susceptible	<i>rrs, whiB7, gidB</i>	nil
Kanamycin	Susceptible	<i>Rv2417c-eis, whiB7, rrs, gidB</i>	nil
Capreomycin	Resistant	<i>tlyA, whiB7, rrs, gidB</i>	<i>tlyA (ins397C)</i>
PAS	Susceptible	<i>ribD, thyA, dfrA, folC</i>	nil
Cycloserine	Susceptible	<i>alr, ddl, cycA</i>	nil

568
569 ONT – Oxford Nanopore Technologies; XDR – Extensively drug resistant; PZA – Pyrazinamide;
570 PAS - Para-amino salicylic acid

571 **Table 2.** Mutations in putative efflux pump/transporter genes identified from ONT assembly of

572 XDR Beijing sub-lineage 2.2.1.1 strain

573

Genes investigated	Gene (mutation) identified	
<i>drrA, drrB, drrC, Rv0194, pstP, efpA, bacA, mmr, Rv1250, Rv1272c, Rv1273c, Rv1634, Rv1258c, mmpL13a, mmpL13b, P55, jefA, Rv0849, Rv2456c, Rv3239c, Rv2994, secA1, pstB, Rv2265, Rv1217, Rv1218c, uspA, Rv2688c, Rv1819, Rv1877, Rv1273c, Rv1458</i>	<i>Rv0194</i>	p.Met74Thr
	<i>Rv0194</i>	p.Pro1098Leu
	<i>secA1</i>	p.Asp699Glu
	<i>uspA</i>	p.Thr54Ser
	<i>uspA</i>	p.Asp67His
	<i>uspA</i>	Val127Leu
	<i>glnQ</i>	p.Met243Leu
	<i>Rv1218c</i>	p.Gln243Arg
	<i>Rv1250</i>	p.Arg278Gly
	<i>Rv2688c</i>	p.Pro156Thr

574

575 ONT – Oxford Nanopore Technologies; XDR - Extensively drug resistant

576

577 **Table 3:** Mutations identified in genes that encode for potential virulence proteins in the XDR

578 Beijing sub-lineage 2.2.1.1 strain

579

Gene	Nucleotide change	Position	Amino acid
<i>mak</i>	T->C	154283	p.Ser18Pro
<i>mce1A</i>	T->G	199470	p.Ser313Ala
<i>mce1D</i>	T->C	203038	p.Ile188Thr
<i>mce1F</i>	T->C	206339	p.Leu370Pro
<i>mce2A</i>	T->C	686972	p.Phe51Ser
<i>mce2F</i>	A->G	694531	p.Asn432Ser
<i>Rv0634c</i>	A->G	731015	p.Tyr7His
<i>mazF3</i>	G->A	1230778	p.Thr65Ile
<i>ephB</i>	G->T	2191498	p.Gly158Trp
<i>mce3A</i>	G->A	2209465	p.Ala47Thr
<i>mce3F</i>	C->A	2216443	p.Ala396Glu
<i>cstA</i>	C->A	3428917	p.Arg559Ser
<i>mce4C</i>	G->T	3916386	p.Arg191Ser
<i>proV</i>	T->C	4204168	p.Asn84Asp
<i>proX</i>	A->G	4205120	p.Leu85Pro
<i>mycP1</i>	T->C	4364046	Thr238Ala

580

581 XDR - Extensively drug resistant

582

583 **Supplementary**

584 **Fig. S1:** A scheme of workflow to generate variants from Oxford Nanopore technologies (ONT)
585 and Illumina reads

586 **Fig. S2:** Dot plot of sequence accuracy between the draft Beijing sub-lineage 2.2.1.1 strain
587 genome and the reference genome H37Rv. The red dots show a forward orientation while blue
588 dots show reverse orientation

589 **Fig. S3:** Plot of sequence and depth coverage for the assembly of 168 PE/PPE family genes
590 using Oxford minion® reads. The marks on the x-axis represent the different 168 PE/PPE family
591 genes while y-axis respective their percentage assembly coverage (red), and read depth (blue).
592 Sample was sequenced to an average of 273x depth

593 **Fig. S4:** Plot of sequence and depth coverage for the assembly of 168 PE/PPE family genes
594 using Illumina reads. The marks on the x-axis represent the different 168 PE/PPE family genes
595 while y-axis respective their percentage assembly coverage (red), and read depth (blue). Sample
596 was sequenced to average 46.3x depth

597 **Fig. S5:** Dot plot of ‘unique region’ accuracy between the draft Beijing sub-lineage 2.2.1.1 strain
598 (x-axis) genome and one of the Beijing reference genomes assembled from PacBio reads (y-
599 axis), genebank accession number AP018035 (HN-321).

600 **Fig. S6:** Protein structure of the PPE family protein predicted using Phyre2 for a 654bp gene
601 sequence with an end 323bp insertion identified within the assembled genome but absent in the
602 reference genome H37Rv.

603 **Table S1:** Details of Oxford Nanopore Technologies (ONT) reads utilized and assembled
604 genome

605 **Table S2:** Number of SNPs and average base coverage identified from different assembled
606 PE/PPE family genes from ONT and Illumina reads

607 **Table S3:** Mutations in genes involved in cell wall biosynthesis identified in the Beijing sub-
608 lineage 2.2.1.1 strain

609 **Table S4:** Blast search results of the gene sequence with insertion confirming the uniqueness of
610 insertion sequence among lineage 2 genomes

611